Biomacromolecules

pubs.acs.org/Biomac

Article

High-Resolution 3D Bioprinting of Photo-Cross-linkable Recombinant Collagen to Serve Tissue Engineering Applications

Liesbeth Tytgat, Agnes Dobos, Marica Markovic, Lana Van Damme, Jasper Van Hoorick, Fabrice Bray, Hugo Thienpont, Heidi Ottevaere, Peter Dubruel, Aleksandr Ovsianikov, and Sandra Van Vlierberghe*

Cite This: *Biomacromolecules* 2020, 21, 3997−4007

Read Online

ACCESS | Metrics & More | Article Recommendations

ABSTRACT: Various biopolymers, including gelatin, have already been applied to serve a plethora of tissue engineering purposes. However, substantial concerns have arisen related to the safety and the reproducibility of these materials due to their animal origin and the risk associated with pathogen transmission as well as batch-to-batch variations. Therefore, researchers have been focusing their attention toward recombinant materials that can be produced in a laboratory with full reproducibility and can be designed according to specific needs (e.g., by introducing additional RGD sequences). In the present study, a recombinant protein based on collagen type I (RCPhC1) was functionalized with photo-cross-linkable methacrylamide (RCPhC1-MA), norbornene (RCPhC1-NB), or thiol (RCPhC1-SH) functionalities to enable high-resolution 3D printing via two-photon polymerization (2PP). The results indicated a clear difference in 2PP processing capabilities between the chain-growth-polymerized RCPhC1-MA and the step-growth-polymerized RCPhC1-NB/SH. More specifically, reduced swelling-related deformations resulting in a superior CAD-CAM mimicry were obtained for the RCPhC1-NB/SH hydrogels. In addition, RCPhC1-NB/SH allowed the processing of the material in the presence of adipose tissue−derived stem cells that survived the encapsulation process and also were able to proliferate when embedded in the printed structures. As a consequence, it is the first time that successful HD bioprinting with cell encapsulation is reported for recombinant hydrogel bioinks. Therefore, these results can be a stepping stone toward various tissue engineering applications.

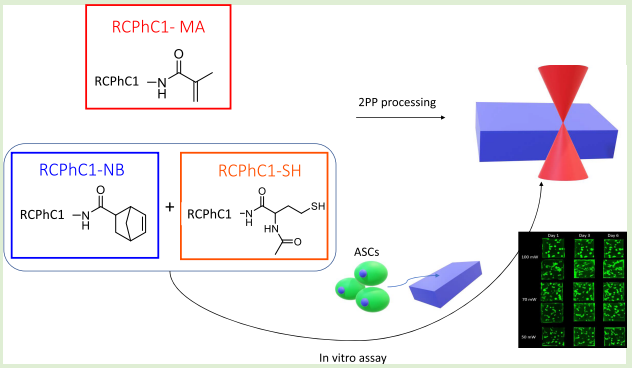

1. INTRODUCTION

Animal-derived gelatin, especially the methacrylamide-modified derivative (Gel-MA), can be considered the gold standard within the field of tissue engineering and biofabrication as reflected by numerous articles published to date.[1−5] However, the use of animal-derived materials has raised increasing concerns due to the occurrence of batch-to-batch variations resulting in issues with reproducibility as well as the possibility for disease transmission toward humans.[6−9] Therefore, researchers have recently shifted their attention toward recombinant proteins as an attractive alternative. As these recombinant materials are produced in a controlled laboratory process, the drawbacks associated with animal-derived materials can be eliminated.[6,7] In literature, both transgenic crops and eukaryotic organisms are described to produce heterotrimeric human recombinant type I collagen, which can be used for tissue engineering purposes.[6,10] Furthermore, recombinant self-assembling peptides can be used as a biomaterial.[11] In the present study, a recombinant protein based on human collagen type I (RCPhC1) was modified to allow the light-based processing of the polymer. RCPhC1 is produced by a yeast fermentation process and contains no animal-derived components. Furthermore, the protein is highly reproducible and is enriched with arginine−glycine−aspartic acid (RGD) tripeptides within its backbone, which contributes to its excellent cell interactivity. Previously, our group has already shown that RCPhC1 can be modified with methacrylamide functionalities.[12] In the present work, we explored the RCPhC1 processing via HD bioprinting using two-photon polymerization (2PP), while the effect of cross-linking chemistry on the 2PP processing capabilities was also evaluated. 2PP is a HD 3D-printing technique that enables the production of scaffolds with a spatial resolution in the submicrometer range due to the nonlinear nature of the 2PP process, thereby often using near-infrared femtosecond pulsed

Received: March 16, 2020
Revised: August 11, 2020
Published: August 25, 2020

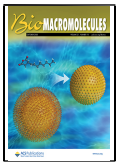

https://dx.doi.org/10.1021/acs.biomac.0c00386
Biomacromolecules 2020, 21, 3997−4007

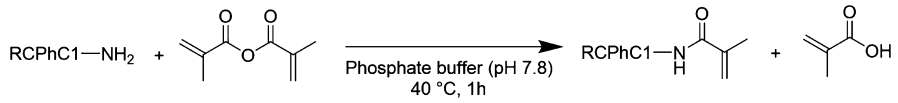

Figure 1. Schematic overview of the modification of RCPhC1 with methacrylamide functionalities (RCPhC1-MA).

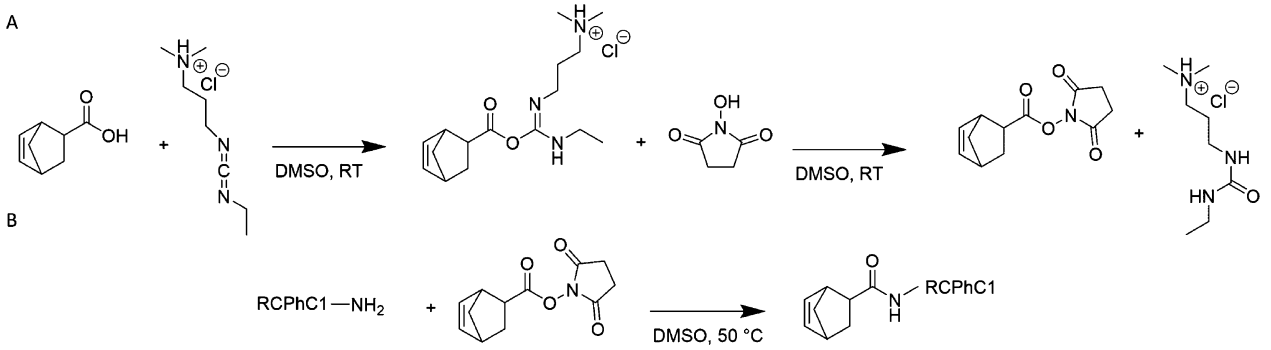

Figure 2. Schematic overview of the development of RCPhC1-NB. (A) Formation of a reactive succinimidyl ester starting from 5-norbornene-2-carboxylic acid. (B) Reaction of the primary amines of RCPhC1-NB with the formed succinimidyl ester to obtain RCPhC1.

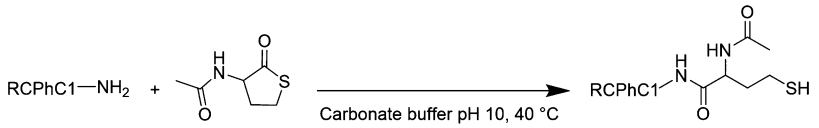

Figure 3. Schematic overview of the development of RCPhC1-SH using *N*-acetyl-homocysteine thiolactone.

laser irradiation.[13] In addition, we also investigated whether the recombinant protein could potentially be applied as a bioink, which implies the production of 3D constructs produced in the presence of living cells.[14] To this end, RCPhC1 was functionalized with different photo-cross-linkable functionalities, including methacrylamide, norbornene, and thiol moieties, which can be cross-linked via chain-growth (methacrylamide) versus step-growth (thiol-norbornene) polymerization in the presence of a suitable photoinitiator upon irradiation using a tightly focused femtosecond laser. In the literature, there are already several reports focusing on 2PP processing of different animal-derived gelatin derivatives including methacrylamide, norbornene, thiol, and methacrylamide-aminoethylmethacrylate moieties.[5,13,15,16] However, to the best of our knowledge, this is the first time that RCPhC1 derivatives are processed via 2PP while exploring their use as a bioink.

2. MATERIALS AND METHODS

2.1. Materials. RCPhC1, commercially available as Cellnest, was kindly provided by Fujifilm Manufacturing Europe B.V. Methacrylic anhydride, 1-ethyl-3-(3-dimethylaminopropyl)carbodiimide (EDC), *N*-acetyl-homocysteine thiolactone, ethylenediaminetetraacetic acid (EDTA), 5-norbornene-2-carboxylic acid, ortho-phthalic dialdehyde (OPA), and sodium hydroxide (NaOH) were purchased from Sigma-Aldrich (Diegem, Belgium). Dimethyl sulfoxide (DMSO), *N*-hydroxysuccinimide (NHS), potassium phosphate monobasic (KH_2PO_4), and sodium phosphate dibasic (Na_2HPO_4) were obtained from Acros Organics (Geel, Belgium). All ^{1}H-NMR spectra were recorded in deuterium oxide (D_2O) purchased from Euriso-top (Saint-Aubin Cedex, France). The photoinitiator tetrapotassium 4,4′-(1,2-ethenediyl)bis[2-(3-sulfophenyl)diazenesulfonate] (DAS) was prepared according to the protocol reported earlier by Tromayer et al.[17] The dialysis membranes, Spectra/Por (molecular weight cutoff (MWCO) 12,000−14,000 g/mol), were obtained from Polylab (Antwerp, Belgium).

2.2. Development and Characterization of RCPhC1-MA, RCPhC1-NB, and RCPhC1-SH. Methacrylamide-modified RCPhC1 (RCPhC1-MA) was developed according to the protocol for Gel-MA published by Tytgat et al.,[12] which is based on the Gel-MA protocol reported by Van Den Bulcke et al.[18] Briefly, a 10 w/v % RCPhC1 (1 g, 0.65 mmol amines) solution was prepared using a 0.1 M phosphate buffer (pH 7.8) at 40 °C. Subsequently, 1 equiv methacrylic anhydride with respect to the number of primary amines present in RCPhC1 was added dropwise to the solution followed by the reaction during 1 h under continuous mechanical stirring at 40 °C (Figure 1). The excess of unreacted methacrylic anhydride together with methacrylic acid formed during the reaction was removed via dialysis (MWCO 12,000−14,000 g/mol) against distilled water for 24 h at 40 °C. Finally, the materials were frozen at −20 °C and lyophilized using a Christ freeze-dryer alpha I-5. ^{1}H-NMR spectroscopy was applied to evaluate whether the modification was successful and to determine the degree of substitution (DS). RCPhC1-MA was dissolved in D_2O and measured at 40 °C using a Bruker Avance (500 MHz) spectrometer.

Norbornene-functionalized RCPhC1 (RCPhC1-NB) was developed using a protocol described earlier by Van Hoorick et al., for norbornene-modified animal-derived gelatin type B (Gel-NB).[16] 5-Norbornene-2-carboxylic acid (2.5 equiv with respect to the primary amines present in RCPhC1) was dissolved in 75 mL dry DMSO at room temperature. Subsequently, 2 equiv EDC and 3 equiv NHS were added to the reaction mixture. The reaction was performed under an inert argon atmosphere during 25 h to form the succinimidyl ester of norbornene (Figure 2). In a next step, the latter solution was heated to 50 °C for 1 h, and 15 g RCPhC1 was dissolved in 225 mL dry DMSO. Subsequently, the mixture containing the succinimidyl ester of norbornene was added to the RCPhC1 solution (12 h, 50 °C, argon atmosphere), allowing the primary amines to react with the succinimidyl ester of norbornene resulting in norbornene-modified RCPhC1 (Figure 2). Afterward, the mixture was precipitated in a tenfold excess of acetone. The precipitate was filtered using a Büchner filter (pore size: 12−15 μm) and washed again with acetone. The remaining residue was dissolved in double-distilled water (resistivity of 18.2 MΩ) and dialyzed against distilled water for 24 h at 40 °C. Finally, the materials were frozen at −20 °C and lyophilized. ^{1}H-NMR spectroscopy was applied to evaluate whether the modification

https://dx.doi.org/10.1021/acs.biomac.0c00386
Biomacromolecules 2020, 21, 3997−4007

was successful and to calculate the DS. RCPhC1-NB was dissolved in D_2O and measured at 40 °C using a Bruker Avance (500 MHz) spectrometer.

Thiolated RCPhC1 (RCPhC1-SH) was developed using a protocol for thiolated animal-derived gelatin (Gel-SH) as reported by Van Vlierberghe et al.[19] Briefly, 10 g RCPhC1 was dissolved under continuous magnetic stirring in a 100 mL carbonate buffer (pH 10) under an inert argon atmosphere (40 °C). To avoid the oxidation of the thiols into disulphide bonds, 1.5 mM EDTA was added to chelate divalent metals present in solution.[20] Subsequently, 5 equiv of *N*-acetyl-homocysteine thiolactone with respect to the primary amines of RCPhC1 was added to the mixture (Figure 3). The solution was allowed to react for 3 h at 40 °C under continuous mechanical stirring. The mixture was dialyzed under an inert argon atmosphere at 40 °C for 24 h using dialysis membranes (Spectra/Por MWCO 12,000−14,000 g/mol). Lastly, the obtained RCPhC1-SH was frozen and lyophilized.

To determine the DS of RCPhC1-SH, a spectrophotometric OPA assay was applied as reported by Tytgat et al.[21] Briefly, a first stock solution was prepared by dissolving 20 mg OPA in 10 mL ethanol and diluting it to 50 mL by adding double-distilled water. Subsequently, a second stock solution was prepared by dissolving 25 μL of 2-mercaptoethanol to 50 mL of a borate buffer (0.1 molar; pH 10). First, a calibration curve was obtained by measuring the absorbance (at 335 nm) of a reference sample (1 mL double-distilled water, 0.5 mL stock solution 1, and 1.5 mL stock solution 2) to a sample containing 50 μL *n*-butylamine standard solutions (0.002 M, 0.006 M, and 0.01 M), 0.95 mL double-distilled water, 0.5 mL stock solution 1, and 1.5 mL stock solution 2. Unmodified RCPhC1 and RCPhC1-SH were dissolved in double-distilled water at a concentration of 25 mg/mL. Next, 50 μL RCPhC1 solution was added to 0.95 mL double-distilled water, 1.5 mL stock solution 2, and 0.5 mL stock solution 1. All measurements were performed in triplicate at 37 °C.

2.3. Molecular Weight Determination Using MALDI-TOF/TOF. The molecular weight (M_W) of pristine RCPhC1 and the RCPhC1 derivatives was measured using an AB SCIEX 4800+ proteomics matrix-assisted laser desorption/ionization time-of-flight (MALDI-TOF/TOF) analyzer (SCIEX, Framingham, MA, USA). The measurements were performed in positive ion linear mode (2000 scans). The material was dissolved in water (1 mg/mL), and 1 μL of each sample was spotted on the target plate and mixed with 1 μL matrix HCCA (10 mg/mL water/ACN (30:70) and 0.1% formic acid).

2.4. Gel Fraction Determination. Gel fraction of 2D hydrogel films was determined on punched out discs (diameter 8 mm). To this end, hydrogel films were made in the presence of 2 mol % Li-TPO and UV cross-linked (30 min UV-A exposure at 10 mW/cm^2). The discs were lyophilized, weighed, and incubated in phosphate buffered saline (PBS) at 37 °C for 24 h. Subsequently, the discs were freeze-dried and weighed again. The gel fraction is defined as follows:

$$\text{Gel fraction} = \frac{\text{Wde}}{\text{Wd0}} \times 100$$

where Wd0 is the freeze-dried weight before swelling and Wde is the freeze-dried weight following equilibrium swelling. These calculations were repeated at least five times per sample.

2.5. Mass Swelling Ratio Determination. Hydrogel films were made as described above and punched out (discs 8 mm diameter). The discs were weighed following 24 h of incubation in PBS for 24 h at 37 °C. Subsequently, the discs were lyophilized and weighed again. The mass swelling ratio was defined as follows:

$$\text{Mass swelling ratio(q)} = \frac{Ws}{Wd},$$

where Ws is the weight of the swollen discs and Wd is the weight of the lyophilized discs following swelling.

2.6. In Situ Rheological Assessment. A rheometer (Physica MCR-301; Anton Paar, Sint-Martens-Latem, Belgium) was used to evaluate the gelation kinetics of the hydrogels. The measurements were done through dynamic oscillation of two parallel plates to determine the storage modulus (G').

Each solution of 300 μL containing 2 mol % Li-TPO-L was placed between the plates with a gap set to 0.3 mm to monitor the UV-induced cross-linking kinetics of the hydrogels in situ. Silicone grease was applied to seal the edges to avoid dehydration of the gel. An oscillation frequency of 1 Hz was applied with a strain of 0.1%. The solutions were cooled to 5 °C to induce physical gelation, which was monitored for 10 min followed by the exposure to UV-A light (EXFO Novacure 2000 UV light source at 365 nm using an intensity of 3500 mW/cm^2) to evaluate the G' of the dual cross-linked hydrogels. The storage modulus of chemically cross-linked hydrogels was determined by exposing the solutions to UV-A light during 440 s at 37 °C.

2.7. 2PP Processing. The 2PP experiments were performed using a previously reported in-house-developed setup.[13] The device consists of a tunable laser (MaiTai eHP DeepSee; Spectra-Physics) delivering 70 fs pulses at a repetition rate of 80 MHz, which is placed behind the 10x/0.3 Zeiss microscope objective (Plan-Apochromat, Oberkochen, Germany). The central wavelength was set to 720 nm for the present experiments. High-resolution printing was obtained using a motorized microscope stage and a dual-axis galvanometric scanner to position the sample and the laser, respectively. The CAD model was sliced with a layer spacing of 0.5 μm and hatched with a 0.5 μm line spacing. The focal spot of the laser was scanned in every layer in a XY alternating fashion. Writing speeds of 100, 500, and 1000 mm/s and average laser powers varying between 10 and 100 mW with 5 mW increments were applied for printing. The 7.5 and 10 w/v % hydrogel precursor solutions containing RCPhC1-MA or RCPhC1-NB/SH in an equimolar thiol-ene concentration and 2 mol % DAS with respect to the photo-cross-linkable functionalities were dissolved in PBS. Approximately 30 μL of each solution was pipetted into a glass bottom dish (μ-Dish, 35 mm; Ibidi) where two glass plates were separated by a 1 mm-thick silicone spacer. The bottom glass plate was functionalized with methacrylate functionalities according to the protocol previously described by Dobos et al. to enable sufficient attachment between the glass and the produced structures.[13] The residual nonpolymerized material was removed using 2 mL PBS followed by incubation of the samples at 37 °C.

2.8. Equilibrium Swelling Assay. Laser scanning microscopy (Zeiss, Oberkochen, Germany) was employed to characterize the postproduction swelling of the materials/hydrogels.[13] For each RCPhC1 derivative, an array of cubes (100 μm × 100 μm × 100 μm) was printed using different laser powers and writing speeds. For every condition, three replicates were produced. The cubes were placed in an incubator at 37 °C to allow equilibrium swelling in PBS (24 h). Fluorescence imaging using a confocal laser scanning microscope was possible after adding 1 mg/mL of 2000 kDa FITC-labeled dextran (TdB Consultancy AB, Sweden) to the PBS solution. Afterward, a semiquantitative swelling ratio was obtained by measuring the surface area of the top of the CAD model (A_{CAD}) and comparing it with the surface area of the top layer of the printed structure (A_{Cube}). The surface swelling ratio was calculated by the following equation:

$$\text{Surface swelling ratio} = \frac{A_{\text{Cube}} - A_{\text{CAD}}}{A_{\text{CAD}}} \times 100 \quad (1)$$

2.9. Direct Cell Encapsulation Using 2PP. A hTERT-immortalized human adipose tissue−derived stem cell line (ASC/TERT1) (Evercyte) was transfected with green fluorescent protein (GFP) to obtain permanently transfected green-labeled cells following a previously established protocol.[22] ASCs-GFP were cultured in endothelial cell growth (EGM-2) media (Lonza) supplemented with 10% fetal bovine serum (Sigma). The cells were maintained in an incubator (high humidity, 5% CO_2, 37 °C), and the medium was changed every second day. To enable printing in the presence of living cells, the cells were trypsinized with 0.5% trypsin−EDTA and resuspended at 1 x 10^6 cells/mL in 7.5 and 10 w/v % RCPhC1-NB/SH solution supplemented with 2 mol % DAS with respect to the photo-cross-linkable functionalities. The solution was pipetted into a

https://dx.doi.org/10.1021/acs.biomac.0c00386
Biomacromolecules 2020, 21, 3997−4007

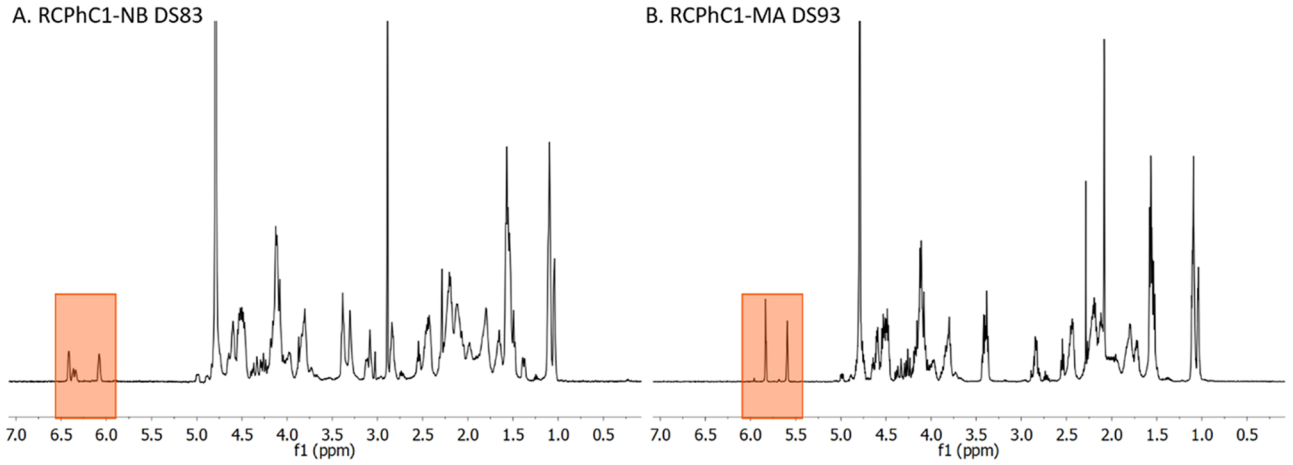

Figure 4. [1]H-NMR spectra of (A) RCPhC1-NB and (B) RCPhC1-MA. The characteristic peaks associated with norbornene (both the endo-form (6.41 and 6.08 ppm) and the exo-form derivatives (6.36 and 6.34 ppm)) and methacrylamide (5.8 and 5.5 ppm, which correspond to the vinyl protons of the methacrylamide functionalities introduced) are highlighted, respectively.

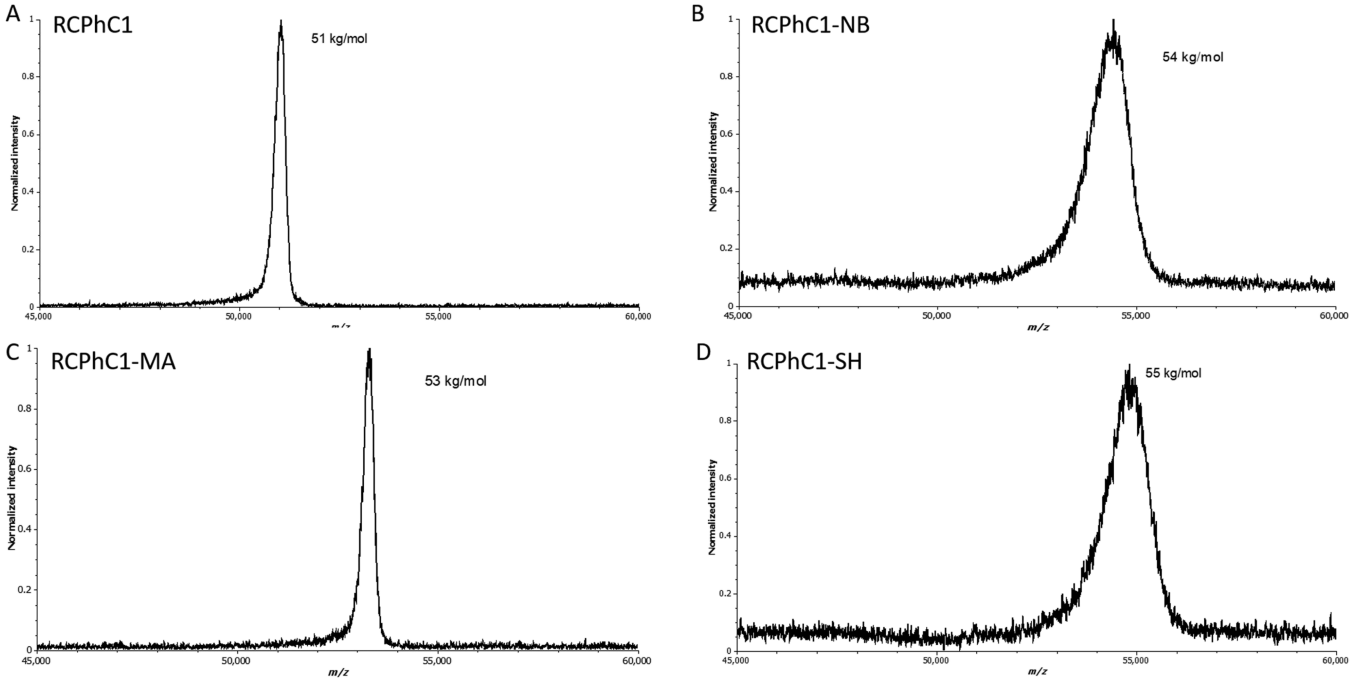

Figure 5. MALDI-TOF/TOF spectra of (A) RCPhC1, (B) RCPhC1-NB, (C) RCPhC1-MA, and (D) RCPhC1-SH.

silicone mold in the glass bottom methacrylated Ibidi dishes. Cubes of 200 μm × 200 μm × 200 μm were printed using a writing speed of 1000 mm/s and laser powers of 50, 70, and 100 mW. The proliferation rate was determined by counting the cells in the cubes after days 1, 3, and 6, and the data were normalized to day 1. To this end, ImageJ software was used to assess maximum intensity imaging of Z-stacks. The cells were manually counted. A total of 4 replicates were used per sample.

2.10. Statistical Analysis. A two-tailed Student t-test was performed when two groups were compared. When more groups were analyzed, statistical analysis was performed using a one-way unifactorial analysis of variance (ANOVA). The values were considered statistically significant, if the p-value was <0.05.

3. RESULTS AND DISCUSSION

3.1. Development and Characterization of RCPhC1 Building Blocks. The different hydrogel precursors were modified to introduce photo-cross-linkable moieties. In summary, the primary amines of RCPhC1 were modified with either norbornene (RCPhC1-NB), or thiol (RCPhC1-SH), or methacrylamide (RCPhC1-MA) functionalities using 5-norbornene-2-carboxylic acid, *N*-acetyl-homocysteine thiolactone, or methacrylic anhydride, respectively, to subsequently enable thiol-ene photoclick (step-growth) or chain-growth polymerization in the presence of a suitable photoinitiator.

[1]H-NMR spectroscopy was applied to determine the DS of RCPhC1-NB and RCPhC1-MA by comparing the characteristic peaks of norbornene (cfr. endo form at 6.41 and 6.08 ppm; exo form at 6.36 and 6.34 ppm) and methacrylamide (cfr. 5.8 and 5.5 ppm) with the reference peak corresponding to the hydrogen atoms of the chemically inert Leu, Ile, and Val amino acids at 1.0 ppm (Figure 4).[16] During the modification of norbornene-functionalized RCPhC1, 2.5 equiv 5-norbornene-2-carboxylic acid, 3 equiv NHS, and 2 equiv EDC were added, yielding 0.55 mmol norbornene groups per gram

https://dx.doi.org/10.1021/acs.biomac.0c00386
Biomacromolecules 2020, 21, 3997−4007

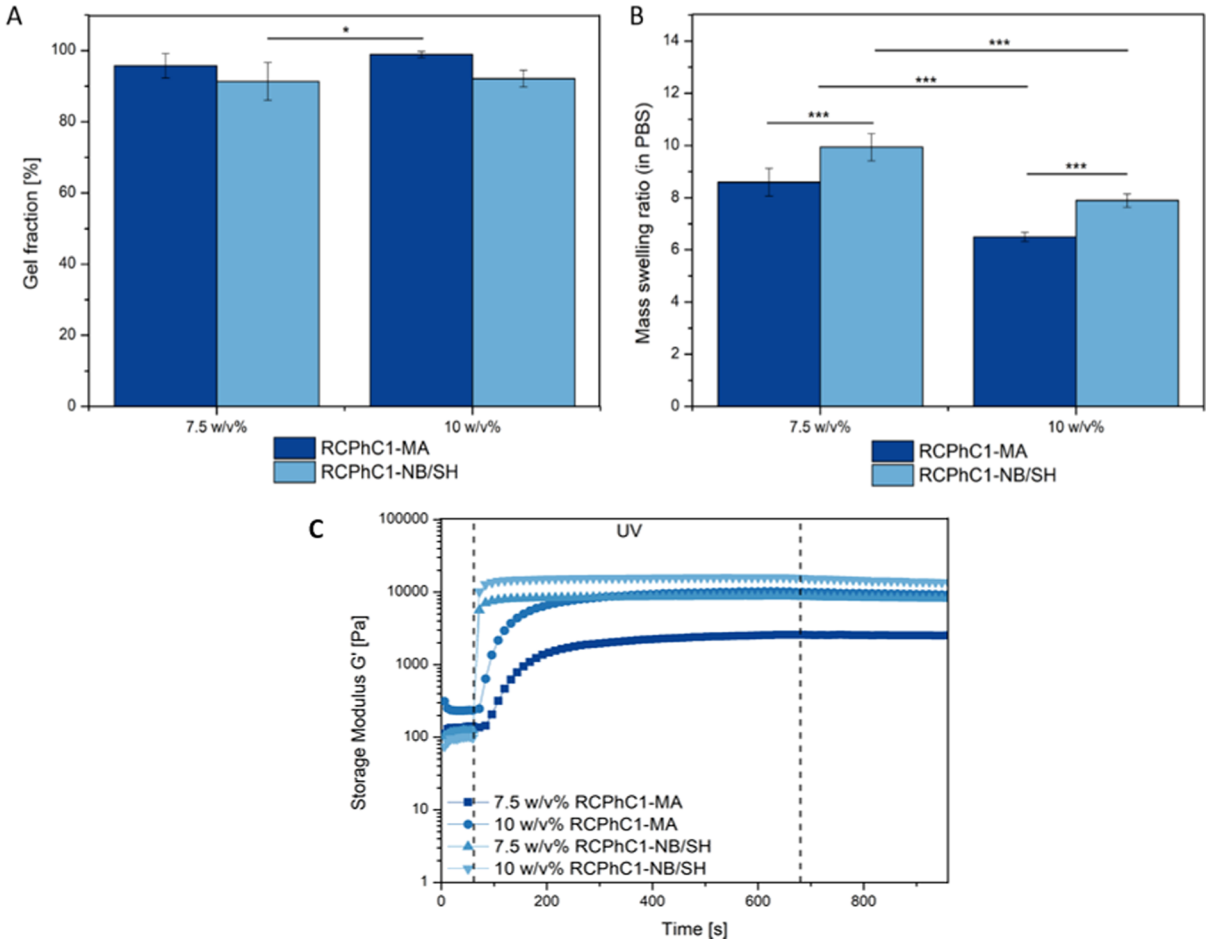

Figure 6. (A) Gel fraction and (B) mass swelling ratio determined in PBS of 7.5 and 10 w/v % RCPhC1-NB/SH and RCPhC1-MA. Significant differences are indicated with an (*) asterisk. (C) In situ photorheology on 7.5 and 10 w/v % solutions of RCPhC1-NB/SH and RCPhC1-MA in the presence of 2 mol % Li-TPO-L at 37 °C.

RCPhC1, which resulted in a DS of 83%. For the development of RCPhC1-MA, 1 equiv methacrylic anhydride was added to the reaction mixture, which resulted in 0.62 mmol double-bond functionalities per gram RCPhC1. The latter corresponds to a DS of 93%.

The DS of thiolated RCPhC1 was calculated using a spectrophotometric assay that was based on the difference between the number of primary amines of RCPhC1 before and after modification using OPA. During the modification, 5 equiv of *N*-acetyl-homocysteine thiolactone was added, resulting in 0.48 mmol thiol groups per gram RCPhC1, corresponding to a DS of 73%.

Furthermore, the M_W of the RCPhC1 derivatives was determined using the MALDI-TOF/TOF analyzer. The results indicated that the M_W of RCPhC1 was 51 kg/mol, while the M_W of RCPhC1-MA, RCPhC1-NB, and RCPhC1-SH was 53, 55, and 55 kg/mol, respectively (Figure 5). The M_W of the RCPhC1 derivatives increased with respect to the starting material RCPhC1 after introducing photo-cross-linkable moieties onto the material backbone. The results indicated that a higher molecular weight (crf. 55 kg/mol) is obtained when more bulky functionalities including norbornene (121 g/mol) and thiol (160 g/mol) groups are incorporated, while for RCPhC1-MA only a molecular weight increase of 2 kg/mol was observed due to the lower molecular weight of the methacrylamide moieties (69 g/mol). These M_W results obtained for the RCPhC1 derivatives are in close accordance with the DS determined via ^{1}H-NMR spectroscopy or the fluorometric assay, taking into account that there are 34 primary amines present in one RCPhC1 chain. The DS, determined via MALDI-TOF/TOF, of RCPhC1-MA, RCPhC1-NB, and RCPhC1-SH is 94, 85, and 67%, respectively. The small differences between the DS can be explained by the fact that for ^{1}H-NMR spectroscopy and the fluorometric OPA assay, the average information is used, whereas MALDI-TOF/TOF provides a more in depth explanation of each of the compound under study. Small deviations can thus be observed as other components can cause deviation of the average DS. Similar observations were already found by Xin et al., who observed changes based on a rise of the molar ratio applied for ^{1}H-NMR spectroscopy results, but no obvious change was seen using the MALDI-TOF/TOF analyzer.[23]

Moreover, a broader peak can be observed for RCPhC1-NB and RCPhC1-SH compared with the RCPhC1-MA (Figure 5). The presence of the broad peak highlights the presence of several forms of the recombinant protein, namely, with a different amount of modified lysines.

3.2. Physicochemical Characterization of the RCPhC1 Derivatives. The gel fraction of the hydrogel films developed was determined in order to evaluate whether stable hydrogels were formed. Similar gel fractions exceeding 90% were

https://dx.doi.org/10.1021/acs.biomac.0c00386
Biomacromolecules 2020, 21, 3997−4007

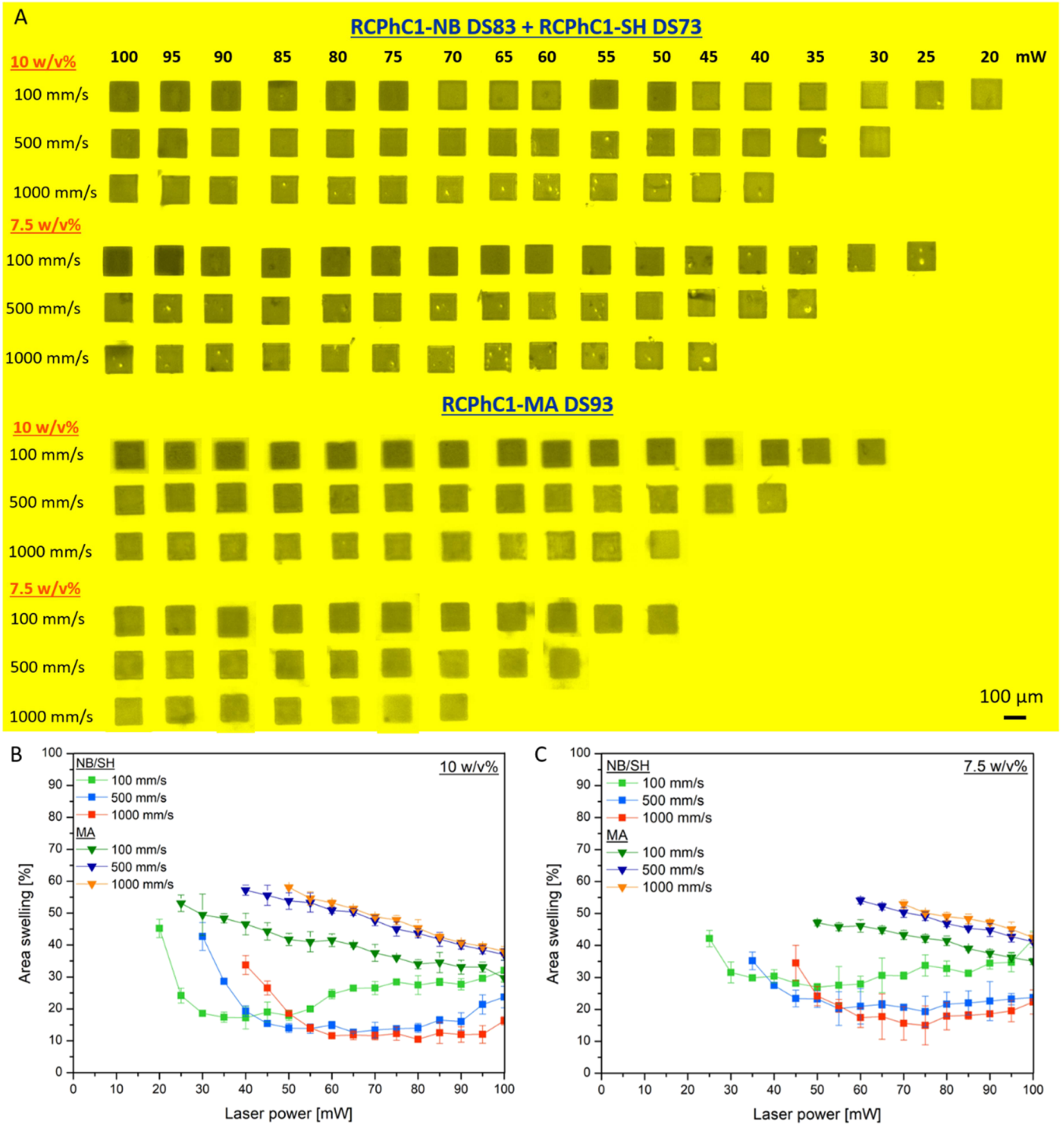

Figure 7. (A) Evaluation of processing window of both RCPhC1 derivatives (7.5 and 10 w/v %) via 3D Z-stacks (maximum projection) of 100 × 100 × 100 μm^3 cubes printed at different laser powers and writing speeds. (B, C) Semiquantitative analysis of the swelling properties of the RCPhC1-NB/SH- (squares) and RCPhC1-MA- (triangles) printed cubes by comparing the surface area of the top layer to the same layer of the CAD model for a concentration of 10 and 7.5 w/v %.

obtained for all hydrogels indicating successful hydrogel film formation. The results are in agreement with the gel fractions reported earlier for the animal-derived gelatin counterparts. For example, Van Nieuwenhove et al. obtained a gel fraction of 98% for 10 w/v % Gel-MA DS95.[24] Furthermore, Van Hoorick et al. observed no significant difference between 5 and 10 w/v % Gel-MA DS97.[15] The water uptake capacity of the hydrogels developed was evaluated to gain insight into their ability to mimic the aqueous environment of the ECM of native tissue. To this end, the equilibrium mass swelling ratio in PBS was determined for the different RCPhC1 derivatives at a concentration of 7.5 and 10 w/v % (Figure 6). The results indicated that all hydrogels were able to absorb large quantities of water. As anticipated, a higher mass swelling ratio was obtained for the hydrogel films produced starting from the lowest RCPhC1 concentration. The latter can be explained by considering the mechanical properties of the hydrogels, which showed that the G' of the hydrogels composed of 7.5 w/v % is

https://dx.doi.org/10.1021/acs.biomac.0c00386
Biomacromolecules 2020, 21, 3997−4007

lower than 10 w/v % hydrogels, implying that a less densely cross-linked network is formed, which is able to absorb more water. In addition, for both concentrations, a significant difference ($p < 0.001$) between the mass swelling ratio of RCPhC1-NB/SH and RCPhC1-MA was observed. The thiol-ene photoclick hydrogels swelled to a greater extent compared with the chain growth cross-linked hydrogels. The latter was also observed earlier for Gel-NB/SH versus Gel-MA scaffolds produced via extrusion-based 3D printing.[21] Herein, the greater swelling properties of the norbornene/thiol hydrogels were attributed to the step-growth polymerization mechanism, which resulted in a more homogeneous network compared with the heterogeneous network based on hydrophobic oligo-methacrylamide chains formed during chain-growth polymerization. Bertlein et al. observed the same trend for their swelling results based on allylated gelatin (Gel-AGE) cross-linked with dithiothreitol (DTT) and compared with Gel-MA hydrogels.[25] They recorded a higher mass swelling ratio for thiol-ene photoclick cross-linked hydrogels versus free-radical conventional chain-growth-polymerized materials.

In situ photorheology experiments were performed in order to evaluate whether step-growth polymerization has an effect on the reactivity and the mechanical properties of the hydrogels compared with chain-growth cross-linked hydrogels. The results indicated that a higher reactivity was obtained for the thiol-ene photoclick hydrogels compared with the RCPhC1-MA hydrogels, revealing a clear benefit of step-growth cross-linking over conventional free-radical cross-linking (Figure 6). The latter is due to the fact that step-growth polymerization is not inhibited by oxygen, which means that the radicals formed can immediately start the cross-linking mechanism and do not have to consume the inhibiting oxygen first as is the case for chain-growth polymerization. These observations are in agreement with the results obtained by Van Hoorick et al., who investigated the reactivity of Gel-NB combined with 0.5 equiv DTT and compared it to Gel-MA DS65.[16]

Furthermore, the results showed that higher storage moduli were obtained when a higher concentration was applied due to the higher number of photo-cross-linkable functionalities present, thereby contributing to a stronger network.[12,26,27] For the concentrations 7.5 and 10 w/v %, the G' of RCPhC1-NB/SH was 8700 and 16,000 Pa, respectively, while they were 2500 and 10,000 Pa for 7.5 and 10 w/v % RCPhC1-MA, respectively (Figure 6). Indeed, the RCPhC1-NB/SH hydrogels formed a stronger network than the RCPhC1-MA hydrogels in the relaxed state (Figure 6). The latter is due to the fact that in step-growth polymerization, each norbornene functionality will only react with one thiol moiety, thereby resulting in a homogeneous network, while on the other hand, in a free-radical chain-growth polymerization, different methacrylamide functionalities will react with each other, thereby forming short oligo-methacrylamide chains resulting in multiple cross-links per junction knot. In addition, the methacrylamide moieties of one chain can also react with each other, thereby creating a heterogeneous and therefore weaker network in the relaxed state. From the literature, it is known that when Gel-NB is cross-linked with a bifunctional thiolated cross-linker, the mechanical properties of the hydrogels are lower than that of Gel-MA.[16] However, when a tetrafunctional thiolated cross-linker is applied, the storage modulus is roughly five times higher, which indicates that increasing the functionality of the cross-linker results in a stronger network.[28] In our study, a multifunctional thiolated cross-linker is used, and therefore, higher storage moduli are obtained compared with those for RCPhC1-MA.

3.3. Optimization of the 2PP Processing Parameters of the RCPhC1 Derivatives. The 2PP structuring performance of RCPhC1-NB combined with RCPhC1-SH in comparison with RCPhC1-MA was evaluated by structuring cubes ($100 \times 100 \times 100\ \mu m^3$) in both material types, dissolved in PBS at different concentrations using DAS as the photoinitiator.[29,30] The processing window was established by printing at different writing speeds (100, 500, and 1000 mm/s) and laser powers (10−100 mW). Due to the applied photoinitiator DAS, a wavelength of 720 nm was used throughout the experiments. Laser scanning microscopy (LSM) is a useful technique to gain semiquantitative insight into the structuring performance and the swelling characteristics of the printed RCPhC1-based structures by comparing the surface area of the top layer to the same layer of the CAD design (Figure 6). The results indicated that both RCPhC1 materials could be processed via 2PP. However, there is a clear difference in processing performance between RCPhC1-NB/SH and RCPhC1-MA. Indeed, upon increasing the writing speed, the structuring threshold increased from 20 to 40 mW for 10 w/v % RCPhC1-NB/SH, while it increased from 30 to 50 mW for the same concentration of RCPhC1-MA, indicating that stable RCPhC1-NB/SH-based structures could be produced with lower laser powers compared with RCPhC1-MA. Van Hoorick et al. observed a similar trend upon printing cubes of animal-derived Gel-MA, Gel-MA-AEMA, and Gel-NB combined with DTT using different polymer concentrations (5−15 w/v %).[15,16] These results are intuitive, as thiol−norbornene reactions are characterized by much lower initiation thresholds (at least 10 times lower than chain-growth polymerization) and fast reaction kinetics due to the absence of reaction conditions, ring strain relief, and a fast proton transfer.[5]

Furthermore, the postproduction swelling assay indicated a lower swelling degree for the structures printed in RCPhC1-NB/SH at each writing speed and concentration compared with RCPhC1-MA, thereby resulting in less swelling-related deformations and thus a superior CAD-CAM mimicry (Figure 7).

Due to postproduction swelling or shrinkage, the CAD model can undergo morphological changes resulting in limitations regarding 3D-printing resolutions. By minimizing these swelling-related deformations, for example, by applying a superior material, a superior, more ideal CAD/CAM mimicry can be obtained and thus no pre-emptive corrections need to be performed to obtain the desired CAD-CAM mimicry.[15,31]

An opposite trend in swelling properties between both materials was observed upon increasing the writing speed. Indeed, for RCPhC1-NB/SH, the cubes printed at 1000 mm/s exhibited a reduced swelling in comparison with the structures printed at 100 mm/s, while for RCPhC1-MA, a higher swelling degree was obtained for constructs printed at 1000 mm/s compared with 100 mm/s (Figure 7B,C). In addition, the results indicated that the swelling degree of the RCPhC1-NB/SH cubes increased at higher laser powers, whereas it decreased for the RCPhC1-MA cubes. We hypothesize that this behavior is a consequence of the cross-linking mechanism. More specifically, one of the characteristics of chain-growth polymerization is the fact that the reaction is inhibited by oxygen. Therefore, more energy is required to produce

https://dx.doi.org/10.1021/acs.biomac.0c00386
Biomacromolecules 2020, 21, 3997−4007

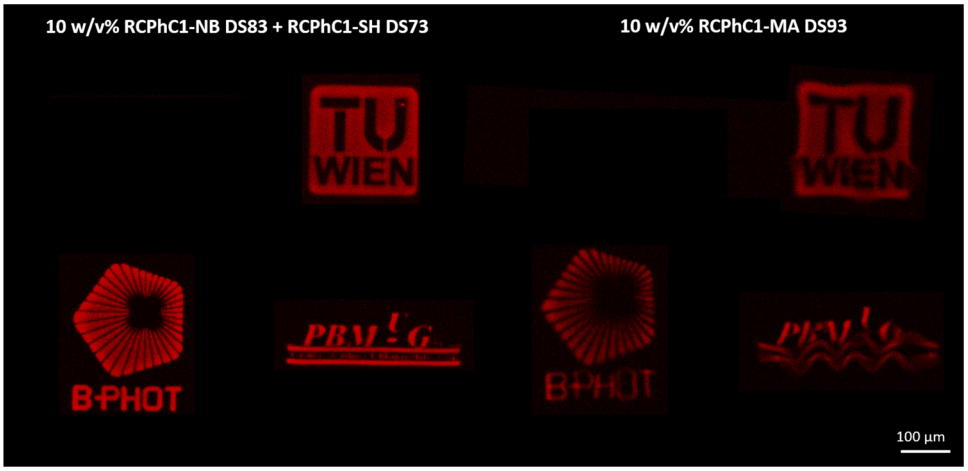

Figure 8. Different logos (TU Wien, B-PHOT, and PBM) were printed starting from 10 w/v % RCPhC1-NB/SH (left panel) versus 10 w/v % RCPhC1-MA (right panel) using a laser power of 70 mW and a writing speed of 1000 mm/s. The logos were reproduced with the permission of TU Wien, B-PHOT, and PBM.

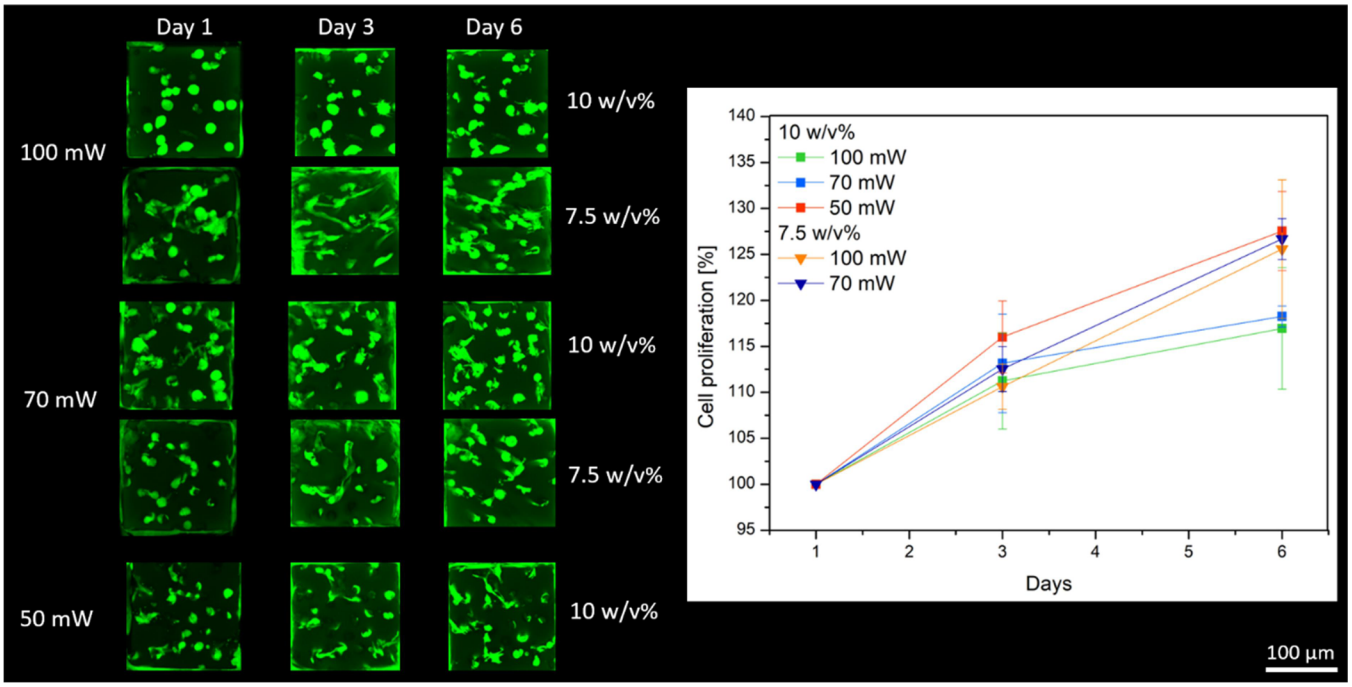

Figure 9. LSM images of 200 × 200 × 200 μm^3 RCPhC1-NB/SH-based cubes printed in the presence of living ASCs-GFP using 2 mol % DAS with respect to the photo-cross-linkable functionalities (left). The cubes were printed using different concentrations and laser powers. Evolution of the cell proliferation as a function of time (right).

sufficient radicals to initiate cross-linking because some of the radicals will be consumed by oxygen. The latter is achieved by printing at lower writing speeds and higher laser powers. On the other hand, step-growth polymerization is not oxygen-inhibited. Therefore, at 100 mm/s and high laser powers, a high amount of energy will be supplied, resulting in the formation of a high number of thiol radicals, which increases the chance of termination reactions to occur between two thiol radicals, thereby resulting in disulfide bonds.[5,13] The latter will lead to a nonequimolar thiol-ene ratio, resulting in a less cross-linked network with a higher swelling degree.[32] Significant differences were observed between RCPhC1-MA and RCPhC1-NB/SH cubes for each laser power assessed in both a 7.5 and 10 w/v % concentration. Furthermore, it could be observed that for higher laser powers (exceeding 50 mW), there were no significant differences observed between the writing speeds of 500 and 1000 mm/s for 10 w/v % cubes for both RCPhC1-MA and RCPhC1-NB/SH. Lastly, similar observations were found for 7.5 w/v % hydrogels. More specifically, when exploiting a laser power of 70 mW or higher, no significant differences were observed at writing speeds of 500 and 1000 mm/s for each of the materials under evaluation.

Furthermore, the difference in swelling properties and thus the CAD-CAM mimicry can also be observed in Figure 8. Several logos were printed in either RCPhC1-NB/SH or RCPhC1-MA using a writing speed of 1000 mm/s and a laser power of 70 mW. The images of the logos obtained via LSM showed a superior CAD-CAM mimicry for the thiol-ene photoclick hydrogels (left panel) in comparison with the chain-growth polymerized materials (right panel).

https://dx.doi.org/10.1021/acs.biomac.0c00386
Biomacromolecules 2020, 21, 3997−4007

3.4. In Vitro Biological Evaluation. The potential of 2PP processing in the presence of living cells was also evaluated using the thiol-ene photoclick hydrogels. This experiment was only performed in this type of hydrogels due to their fast cross-linking kinetics and their excellent CAD-CAM mimicry. To this end, cubes of 200 × 200 × 200 μm^3 were printed at high writing speeds, i.e., 1000 mm/s, using DAS that is a suitable photoinitiator for direct cell encapsulation using 2PP.[17] RCPhC1-NB/SH was processed together with GFP-labeled ASCs to evaluate the potential of the RCPhC1 derivative to function as a bioink. The results indicated that the cells survived the printing process and were able to proliferate within the printed hydrogel, which is also observed by Dobos et al. (Figure 9).[13] They showed that L929 mouse fibroblasts in 7.5 w/v % animal-derived Gel-NB combined with equimolar amounts of DTT also survived the 2PP encapsulation process and started to proliferate over time, obtaining their desired morphology.[13] These findings are correlated to the material stiffness with softer materials, resulting in an increased proliferation and extended morphology of the fibroblasts.[13] In addition, the cells were able to proliferate to a higher extent in the cubes formed starting from a 7.5 w/v % polymer concentration in comparison with the 10 w/v % concentration. However, no significant differences were found. Furthermore, when assessing the fluorescence images, it can be observed that the cells mimic their innate stretched morphology to a greater extent in 7.5 w/v % hydrogels. The latter is due to the fact that a less densely cross-linked network is formed using a lower polymer concentration, which results in a higher proliferation and migration rate.[33−35]

Overall, based on these results, recombinant proteins can offer a promising alternative for animal-derived materials. Bearing in mind that the cost of these recombinant structures is currently one of the limiting factors, research has been focused on increasing the yield and investigating different pathways to produce the recombinant proteins, such as transgenic crops and the use of eukaryotic cells (such as yeasts).[8−10] Furthermore, advances in DNA manipulation have been observed with the introduction of CRISPR,[36] giving rise to a potential cost reduction of these recombinant proteins in the future.

4. CONCLUSIONS

The present study reports on the influence of chain- versus step-growth polymerization by investigating the 2PP processing capabilities of functionalized recombinant RCPhC1 hydrogels along with the materials' potential to become 2PP processed in the presence of living cells. A clear difference in 2PP processing capability was observed between both RCPhC1 derivatives. Indeed, reduced swelling-related deformations and thus a superior CAD-CAM mimicry were obtained for RCPhC1-NB/SH, in contrast with RCPhC1-MA. Furthermore, the swelling properties were also influenced by the concentration, the writing speed, and the irradiation dose applied. In addition, RCPhC1-NB/SH could be processed in the presence of ASCs-GFP that survived the encapsulation process and were able to proliferate inside the printed structures. It can thus be concluded that the RCPhC1-NB/SH hydrogels developed are processable via 2PP and prove to be a perfect bioink alternative to the conventional animal-derived equivalents to serve tissue engineering applications.

AUTHOR INFORMATION

Corresponding Author

Sandra Van Vlierberghe − *Brussels Photonics (B-PHOT) − Department of Applied Physics and Photonics, Vrije Universiteit Brussel and Flanders Make, 1050 Brussels, Belgium; Polymer Chemistry & Biomaterials Group − Centre of Macromolecular Chemistry (CMaC) − Department of Organic and Macromolecular Chemistry, Ghent University, 9000 Ghent, Belgium*; orcid.org/0000-0001-7688-1682; Email: Sandra.VanVlierberghe@UGent.be

Authors

Liesbeth Tytgat − *Brussels Photonics (B-PHOT) − Department of Applied Physics and Photonics, Vrije Universiteit Brussel and Flanders Make, 1050 Brussels, Belgium; Polymer Chemistry & Biomaterials Group − Centre of Macromolecular Chemistry (CMaC) − Department of Organic and Macromolecular Chemistry, Ghent University, 9000 Ghent, Belgium*

Agnes Dobos − *3D Printing and Biofabrication Group, Institute of Materials Science and Technology, 1060 Vienna, Austria; Austrian Cluster for Tissue Regeneration, 1200 Vienna, Austria*

Marica Markovic − *3D Printing and Biofabrication Group, Institute of Materials Science and Technology, 1060 Vienna, Austria; Austrian Cluster for Tissue Regeneration, 1200 Vienna, Austria*

Lana Van Damme − *Polymer Chemistry & Biomaterials Group − Centre of Macromolecular Chemistry (CMaC) − Department of Organic and Macromolecular Chemistry, Ghent University, 9000 Ghent, Belgium*

Jasper Van Hoorick − *Brussels Photonics (B-PHOT) − Department of Applied Physics and Photonics, Vrije Universiteit Brussel and Flanders Make, 1050 Brussels, Belgium; Polymer Chemistry & Biomaterials Group − Centre of Macromolecular Chemistry (CMaC) − Department of Organic and Macromolecular Chemistry, Ghent University, 9000 Ghent, Belgium*

Fabrice Bray − *Miniaturisation pour l'Analyse, la Synthèse et la Protéomique, USR 3290 Centre National de la Recherche Scientifique, University of Lille, Villeneuve d'Ascq 59650, France*

Hugo Thienpont − *Brussels Photonics (B-PHOT) − Department of Applied Physics and Photonics, Vrije Universiteit Brussel and Flanders Make, 1050 Brussels, Belgium*

Heidi Ottevaere − *Brussels Photonics (B-PHOT) − Department of Applied Physics and Photonics, Vrije Universiteit Brussel and Flanders Make, 1050 Brussels, Belgium*

Peter Dubruel − *Polymer Chemistry & Biomaterials Group − Centre of Macromolecular Chemistry (CMaC) − Department of Organic and Macromolecular Chemistry, Ghent University, 9000 Ghent, Belgium*

Aleksandr Ovsianikov − *3D Printing and Biofabrication Group, Institute of Materials Science and Technology, 1060 Vienna, Austria; Austrian Cluster for Tissue Regeneration, 1200 Vienna, Austria*

Complete contact information is available at: https://pubs.acs.org/10.1021/acs.biomac.0c00386

Notes

The authors declare no competing financial interest.

https://dx.doi.org/10.1021/acs.biomac.0c00386
Biomacromolecules 2020, 21, 3997−4007

■ ACKNOWLEDGMENTS

The authors thank Mr. Tim Courtin for his assistance in recording the ^{1}H-NMR spectra. L.T. and J.V. H. acknowledge the Research Foundation Flanders (FWO) for providing them a PhD research fellowship (1S26616N & 1S44016N). S.V. V. thanks the FWO for financial support in the form of research grants (G005616N, G0F0516N, FWOKN273, and G044516N). A.O. acknowledges the financial support from the Austrian Science Funds (FWF Project No. I2444-N28). F.B. acknowledges the IBISA network for the financial support of the USR 3290 (MSAP) proteomics facility. The authors thank Dr. Severin Muehleder (Ludwig Boltzmann Institute for Experimental and Clinical Traumatology, Wien, Austria) for preforming GFP cell transfection.

■ REFERENCES

(1) Yue, K.; Li, X.; Schrobback, K.; Sheikhi, A.; Annabi, N.; Leijten, J.; Zhang, W.; Zhang, Y. S.; Hutmacher, D. W.; Klein, T. J.; Khademhosseini, A. Structural Analysis of Photocrosslinkable Methacryloyl-Modified Protein Derivatives. *Biomaterials* **2017**, *139*, 163−171.

(2) Eke, G.; Mangir, N.; Hasirci, N.; MacNeil, S.; Hasirci, V. Development of a UV Crosslinked Biodegradable Hydrogel Containing Adipose Derived Stem Cells to Promote Vascularization for Skin Wounds and Tissue Engineering. *Biomaterials* **2017**, *129*, 188−198.

(3) Nichol, J. W.; Koshy, S. T.; Bae, H.; Hwang, C. M.; Yamanlar, S.; Khademhosseini, A. Cell-Laden Microengineered Gelatin Methacrylate Hydrogels. *Biomaterials* **2010**, *31*, 5536−5544.

(4) Yue, K.; Trujillo-De Santiago, G.; Moisés Alvarez, M.; Tamayol, A.; Annabi, N.; Khademhosseini, A. Synthesis, Properties, and Biomedical Applications of Gelatin Methacryloyl (GelMA) Hydrogels. *Biomaterials* **2015**, *73*, 254−271.

(5) Van Hoorick, J.; Tytgat, L.; Dobos, A.; Ottevaere, H.; Van Erps, J.; Thienpont, H.; Ovsianikov, A.; Dubruel, P.; Van Vlierberghe, S. (Photo-)Crosslinkable Gelatin Derivatives for Biofabrication Applications. *Acta Biomater.* **2019**, *97*, 46−73.

(6) Pawelec, K. M.; Kluijtmans, S. G. J. M. Biomineralization of Recombinant Peptide Scaffolds: Interplay among Chemistry, Architecture, and Mechanics. *ACS Biomater. Sci. Eng.* **2017**, *3*, 1100−1108.

(7) Olsen, D.; Yang, C.; Bodo, M.; Chang, R.; Leigh, S.; Baez, J.; Carmichael, D.; Perälä, M.; Hämäläinen, E. R.; Jarvinen, M.; Polarek, J. Recombinant Collagen and Gelatin for Drug Delivery. *Adv. Drug Delivery Rev.* **2003**, *55*, 1547−1567.

(8) Wang, T.; Lew, J.; Premkumar, J.; Poh, C. L.; Win Naing, M. Production of Recombinant Collagen: State of the Art and Challenges. *Eng. Biol.* **2017**, *1*, 18−23.

(9) Báez, J.; Olsen, D.; Polarek, J. W. Recombinant Microbial Systems for the Production of Human Collagen and Gelatin. *Appl. Microbiol. Biotechnol.* **2005**, *69*, 245−252.

(10) Stein, H.; Wilensky, M.; Tsafrir, Y.; Rosenthal, M.; Amir, R.; Avraham, T.; Ofir, K.; Dgany, O.; Yayon, A.; Shoseyov, O. Production of Bioactive, Post-Translationally Modified, Heterotrimeric, Human Recombinant Type-I Collagen in Transgenic Tobacco. *Biomacromolecules* **2009**, *10*, 2640−2645.

(11) Kyle, S.; Aggeli, A.; Ingham, E.; McPherson, M. J. Recombinant Self-Assembling Peptides as Biomaterials for Tissue Engineering. *Biomaterials* **2010**, *31*, 9395−9405.

(12) Tytgat, L.; Markovic, M.; Qazi, T. H.; Vagenende, M.; Bray, F.; Martins, J. C.; Rolando, C.; Thienpont, H.; Ottevaere, H.; Ovsianikov, A.; Dubruel, P.; Van Vlierberghe, S. Photo-Crosslinkable Recombinant Collagen Mimics for Tissue Engineering Applications. *J. Mater. Chem. B* **2019**, *7*, 3100−3108.

(13) Dobos, A.; Van Hoorick, J.; Steiger, W.; Gruber, P.; Markovic, M.; Andriotis, O. G.; Rohatschek, A.; Dubruel, P.; Thurner, P. J.; Van Vlierberghe, S.; Baudis, S.; Ovsianikov, A. Thiol−Gelatin−Norbornene Bioink for Laser-Based High-Definition Bioprinting. *Adv. Healthcare Mater.* **2019**, *9*, 1900752.

(14) Levato, R.; Visser, J.; Planell, J. A.; Engel, E.; Malda, J.; Mateos-Timoneda, M. A. Biofabrication of Tissue Constructs by 3D Bioprinting of Cell-Laden Microcarriers. *Biofabrication* **2014**, *6*, 035020.

(15) Van Hoorick, J.; Gruber, P.; Markovic, M.; Tromayer, M.; Van Erps, J.; Thienpont, H.; Liska, R.; Ovsianikov, A.; Dubruel, P.; Van Vlierberghe, S. Cross-Linkable Gelatins with Superior Mechanical Properties Through Carboxylic Acid Modification: Increasing the Two-Photon Polymerization Potential. *Biomacromolecules* **2017**, *18*, 3260−3272.

(16) Van Hoorick, J.; Gruber, P.; Markovic, M.; Rollot, M.; Graulus, G. J.; Vagenende, M.; Tromayer, M.; Van Erps, J.; Thienpont, H.; Martins, J. C.; Baudis, S.; Ovsianikov, A.; Dubruel, P.; Van Vlierberghe, S. Highly Reactive Thiol-Norbornene Photo-Click Hydrogels: Toward Improved Processability. *Macromol. Rapid Commun.* **2018**, *39*, 1−7.

(17) Tromayer, M.; Dobos, A.; Gruber, P.; Ajami, A.; Dedic, R.; Ovsianikov, A.; Liska, R. A Biocompatible Diazosulfonate Initiator for Direct Encapsulation of Human Stem Cells: Via Two-Photon Polymerization. *Polym. Chem.* **2018**, *9*, 3108−3117.

(18) Van Den Bulcke, A. I.; Bogdanov, B.; De Rooze, N.; Schacht, E. H.; Cornelissen, M.; Berghmans, H. Structural and Rheological Properties of Methacrylamide Modified Gelatin Hydrogels. *Biomacromolecules* **2000**, *1*, 31−38.

(19) Van Vlierberghe, S.; Schacht, E.; Dubruel, P. Reversible Gelatin-Based Hydrogels: Finetuning of Material Properties. *Eur. Polym. J.* **2011**, *47*, 1039−1047.

(20) Kudryavtseva, E.; Sidorova, M.; Ovchinnikov, M.; Bespalova, D.; Bushuev, V. Comparative Evaluation of Different Methods for Disulfide Bond Formation in Synthesis of the HIV-2 Antigenic Determinant. *J. Pept. Res.* **1997**, *49*, 52−58.

(21) Tytgat, L.; Van Damme, L.; Van Hoorick, J.; Declercq, H.; Thienpont, H.; Ottevaere, H.; Blondeel, P.; Dubruel, P.; Van Vlierberghe, S. Additive Manufacturing of Photo-Crosslinked Gelatin Scaffolds for Adipose Tissue Engineering. *Acta Biomater.* **2019**, *94*, 340−350.

(22) Knezevic, L.; Schaupper, M.; Mühleder, S.; Schimek, K.; Hasenberg, T.; Marx, U.; Priglinger, E.; Redl, H.; Holnthoner, W. Engineering Blood and Lymphatic Microvascular Networks in Fibrin Matrices. *Front. Bioeng. Biotechnol.* **2017**, *5*, 1−12.

(23) Xin, Y.; Wang, H.; Liu, B.; Yuan, J. Synthesis and MALDI-TOF Characterization of β-CD Core ATRP Initiators and RAFT Chain Transfers with Different Degrees of Substitution. *Chinese J. Polym. Sci. (English Ed.)* **2015**, *33*, 36−48.

(24) Van Nieuwenhove, I.; Salamon, A.; Peters, K.; Graulus, G. J.; Martins, J. C.; Frankel, D.; Kersemans, K.; De Vos, F.; Van Vlierberghe, S.; Dubruel, P. Gelatin- and Starch-Based Hydrogels. Part A: Hydrogel Development, Characterization and Coating. *Carbohydr. Polym.* **2016**, *152*, 129−139.

(25) Bertlein, S.; Brown, G.; Lim, K. S.; Jungst, T.; Boeck, T.; Blunk, T.; Tessmar, J.; Hooper, G. J.; Woodfield, T. B. F.; Groll, J. Thiol − Ene Clickable Gelatin : A Platform Bioink for Multiple 3D Biofabrication Technologies. *Adv. Mater.* **2017**, *29*, 1703404.

(26) Graulus, G.-J.; Mignon, A.; Van Vlierberghe, S.; Declercq, H.; Fehér, K.; Cornelissen, M.; Martins, J. C.; Dubruel, P. Cross-Linkable Alginate-Graft-Gelatin Copolymers for Tissue Engineering Applications. *Eur. Polym. J.* **2015**, *72*, 494−506.

(27) Tytgat, L.; Vagenende, M.; Declercq, H.; Martins, J. C.; Thienpont, H.; Ottevaere, H.; Dubruel, P.; Van Vlierberghe, S. Synergistic Effect of κ-Carrageenan and Gelatin Blends towards Adipose Tissue Engineering. *Carbohydr. Polym.* **2018**, *189*, 1−9.

(28) Munoz, Z.; Shih, H.; Lin, C.-C. Gelatin Hydrogels Formed by Orthogonal Thiol-Norbornene Photochemistry for Cell Encapsulation. *Biomater. Sci.* **2014**, *2*, 1063−1072.

(29) Dobos, A.; Steiger, W.; Theiner, D.; Gruber, P.; Lunzer, M.; Van Hoorick, J.; Van Vlierberghe, S.; Ovsianikov, A. Screening of

https://dx.doi.org/10.1021/acs.biomac.0c00386
Biomacromolecules 2020, 21, 3997−4007

Two-Photon Activated Photodynamic Therapy Sensitizers Using a 3D Osteosarcoma Model. *Analyst* **2019**, *144*, 3056−3063.
(30) Steiger, W.; Gruber, P.; Theiner, D.; Dobos, A.; Lunzer, M.; Van Hoorick, J.; Van Vlierberghe, S.; Liska, R.; Ovsianikov, A. Fully Automated Z-Scan Setup Based on a Tunable Fs-Oscillator. *Opt. Mater. Express* **2019**, *9*, 3567.
(31) Torgersen, J.; Mironov, A. O. V.; Pucher, N.; Qin, X.; Li, Z.; Cicha, K.; Machacek, T.; Liska, R.; Jantsch, V.; Stampfl, J. Photo-Sensitive Hydrogels for Three- Dimensional Laser Microfabrication in the Presence of Whole Organisms. *J. Biomed. Opt.* **2012**, *17*, 15−18.
(32) Pereira, R. F.; Bártolo, P. J. 3D Photo-Fabrication for Tissue Engineering and Drug Delivery. *Engineering* **2015**, *1*, 90−112.
(33) Liu, W.; Heinrich, M. A.; Zhou, Y.; Akpek, A.; Hu, N.; Liu, X.; Guan, X.; Zhong, Z.; Jin, X.; Khademhosseini, A.; Zhang, Y. S. Extrusion Bioprinting of Shear-Thinning Gelatin Methacryloyl Bioinks. *Adv. Healthcare Mater.* **2017**, *6*, 1−11.
(34) Gu, Y.; Zhang, L.; Du, X.; Fan, Z.; Wang, L.; Sun, W.; Cheng, Y.; Zhu, Y.; Chen, C. Reversible Physical Crosslinking Strategy with Optimal Temperature for 3D Bioprinting of Human Chondrocyte-Laden Gelatin Methacryloyl Bioink. *J. Biomater. Appl.* **2018**, *33*, 609−618.
(35) Malda, J.; Visser, J.; Melchels, F. P.; Jüngst, T.; Hennink, W. E.; Dhert, W. J. A.; Groll, J.; Hutmacher, D. W. 25th Anniversary Article: Engineering Hydrogels for Biofabrication. *Adv. Mater.* **2013**, *25*, 5011−5028.
(36) Grav, L. M.; Karottki, K. J. C.; Lee, J. S.; Kildegaard, H. F. Application of CRISPR/Cas9 Genome Editing to Improve Recombinant Protein Production in CHO Cells. *Methods Mol. Biol.* **2017**, *1603*, 101−118.

https://dx.doi.org/10.1021/acs.biomac.0c00386
Biomacromolecules 2020, 21, 3997−4007